

Free vibration analysis of nonlinear resilient impact dampers

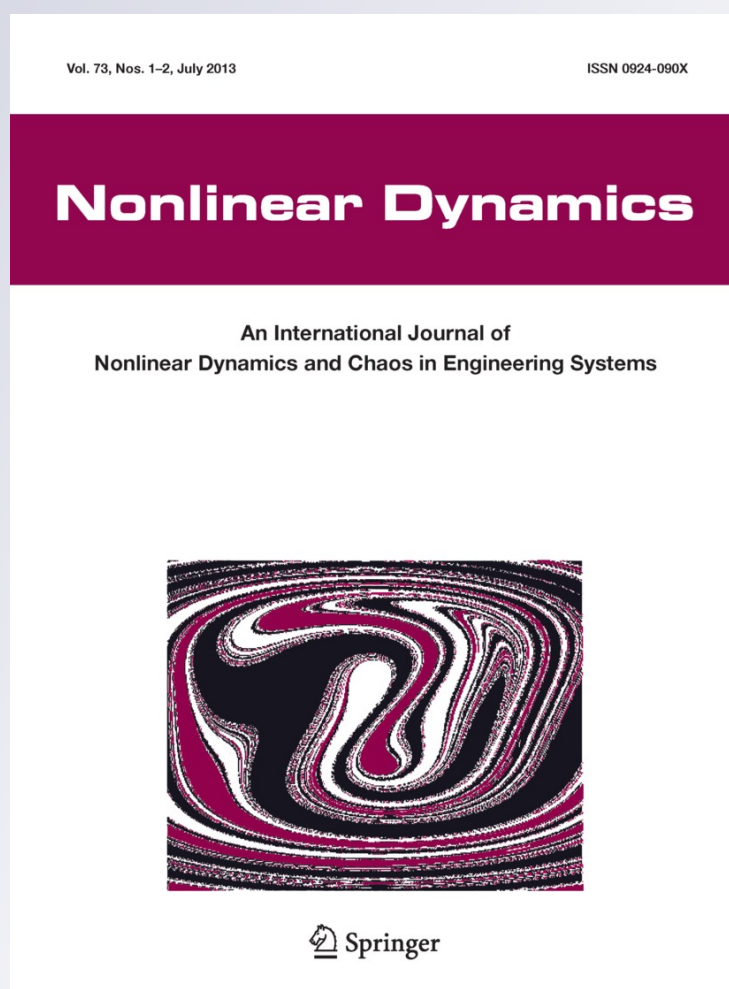
**Aref Afsharfard & Anooshiravan
Farshidianfar**

Nonlinear Dynamics

An International Journal of Nonlinear
Dynamics and Chaos in Engineering
Systems

ISSN 0924-090X
Volume 73
Combined 1-2

Nonlinear Dyn (2013) 73:155-166
DOI 10.1007/s11071-013-0775-1



Your article is protected by copyright and all rights are held exclusively by Springer Science +Business Media Dordrecht. This e-offprint is for personal use only and shall not be self-archived in electronic repositories. If you wish to self-archive your article, please use the accepted manuscript version for posting on your own website. You may further deposit the accepted manuscript version in any repository, provided it is only made publicly available 12 months after official publication or later and provided acknowledgement is given to the original source of publication and a link is inserted to the published article on Springer's website. The link must be accompanied by the following text: "The final publication is available at link.springer.com".

Free vibration analysis of nonlinear resilient impact dampers

Aref Afsharfard · Anooshiravan Farshidianfar

Received: 5 August 2012 / Accepted: 10 January 2013 / Published online: 29 January 2013
© Springer Science+Business Media Dordrecht 2013

Abstract In the present study, free vibration of a vibratory system equipped with an impact damper, which incorporates the Hertzian contact theory, is investigated. A nonlinear model of an impact damper is constructed using spring, mass, and viscous damper. To increase accuracy of the solution, deformation of the impact damper during the collision with and the main mass is considered. The governing coupled nonlinear differential equations of a cantilever beam equipped with the impact damper are solved using the parameter expanding perturbation method. Contact durations, which are obtained using the presented method, are compared with previous results. Gap sizes of the impact dampers are classified to two main parts. The effects of selecting the gap sizes regarding to the discussed classification are investigated on the application of the impact dampers. Based on types of collision between colliding masses, the so-called “effectiveness” is defined. Finally, it is shown variation of the damping inclination with the gap size is similar to variation of the effectiveness.

Keywords Resilient impact damper · Hertzian contact theory · Perturbation method · Damping inclination · Effectiveness

1 Introduction

For many years, researchers have extensively investigated mechanical systems whose elements collide with each other during operation because impacts occur very often in many modern technical devices [1–5]. An impact damper is a small loose mass within a main mass. There are many advantages in using impact dampers over traditional passive devices: They are inexpensive, simple in design, robust and effective in harsh environments with a wide range of frequencies [6]. Applications of the impact dampers to reduce undesired vibrations of turbine blades, machine tools have been investigated [7–10]. It is shown the impact dampers would operate more efficiently than classical dynamic vibration dampers [11]. Bapat and Sankar showed that the coefficient of restitution has a great effect on the performance of impact dampers [12]. They demonstrated that in the case of single unit impact dampers, optimized parameters at resonance are not necessarily optimal at other frequencies. Popplewell and Liao introduced an accurate approximation to determine the optimum clearance of a rigid damper [8]. Ema and Marui investigated the characteristics of an impact damper in free damped vibration [13]. They indicated that the damping capability of the vibratory system could be significantly improved using a proper impact damper. Cheng and Xu obtained a relation between coefficient of restitution and impact damping ratio [14]. They showed that the optimal initial displacement is a monotonically increasing function of damp-

A. Afsharfard (✉) · A. Farshidianfar
Department of Mechanical Engineering,
Ferdowsi University of Mashhad, Mashhad, Iran
e-mail: aref.afsharfard@gmail.com

ing. Son et al. proposed active momentum exchange impact dampers to suppress the first large peak value of the acceleration response due to a shock load [15]. They showed that increasing the coefficient of restitution may lead to increase the reliability of the vibratory systems. Andreus et al. studied a friction oscillator colliding with an obstacle, which is excited by a moving base with constant velocity. They showed the system response both for a rigid and deformable stop using the so-called “friction-impact” map [16]. They also investigated the influence of contact spring rigidity and the ratio between the first natural frequencies of beam and rod, on the system response. They presented the velocity diagrams, nonlinear resonance curves and phase portraits for determining the regions of periodic motion with impacts and the appearance of chaotic solutions, and parameter ranges where the functionality of the non-structural element is at risk [17].

Although the impact damper has been investigated in the past, there are still several shortcomings in this area of research that need to be addressed. For example, in most of previous investigations the period that the impact mass stays in contact with the main mass is assumed negligible. This assumption is reasonable in rigid impact dampers but in case of the resilient impact dampers the contact duration should be accounted. Furthermore, it should be noted the vibro-impact systems often show strongly nonlinear behavior but there is a large tendency for describing these systems using linear equations. To the best of our knowledge, there has been no consideration towards investigating the behavior of nonlinear resilient impact dampers, and hence the main thrust of this paper lies in this subject.

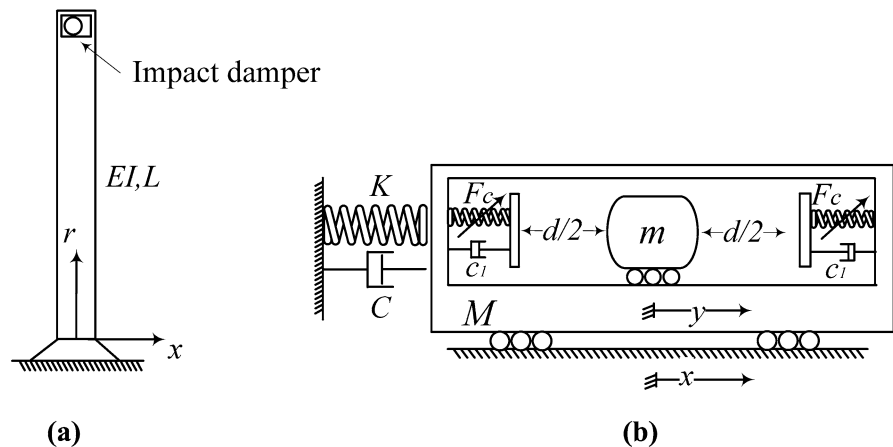
In the present study, dynamic equations of the vibratory motion of a cantilever beam equipped with an impact damper are derived. The governing equations of motion (when contact occurs) are theoretically investigated using the parameter expanding perturbation. The contact duration is calculated and it is compared with previous analytical results. To illustrate the theoretical prediction, a numerical example of the presented vibro-impact system is given. Regarding to the relative motion of colliding masses, the gap sizes are classified to “in range” and “out of the range” gap sizes. Effects of using the discussed class of gap sizes on the damping inclination of the impact damper are studied. Finally, based on the number of effective impacts a new parameter will be introduced, which can predict behavior of the damping inclination.

2 Modeling a vibratory system equipped with an impact damper

2.1 Modeling the elastic beam

Figure 1a shows a cantilever beam equipped with an impact damper. The elastic beam is a continuum with an infinite number of degrees of freedom [18, 19]. The transverse vibratory behavior of the beam can be modeled using a linear spring. The vibratory model of the beam equipped with the impact damper is illustrated in Fig. 1b. As shown in this figure, an impact damper with impact mass m , clearance d ; and oscillator with linear stiffness K , main mass M and viscous damping C is considered. The viscous damper c_1 is added to model accounting for the contact loss.

Fig. 1 Schematic diagram of the beam with an impact damper (a); and Schematic diagram of the impact damper (b)



Parameters K and M can be derived using the Ritz method. In doing so, the Euler–Lagrange partial differential equation of the beam motion, for constant EI , is as follows [20, 21]:

$$\rho A \frac{\partial^2 x}{\partial t^2} + EI \frac{\partial^4 x}{\partial r^4} = f(r, t) \tag{1}$$

where x is the transverse displacement of the beam, E is the Young modulus, ρ is the mass density, A is cross sectional area of the beam and I is the beam moment of inertia. The above equation can be solved using the method of Ritz in conjunction with the principle of virtual displacements [20–22]. Truncated series involving a complete set of basis function, which can be used to show the displacements, is given by

$$x(r, t) = \sum_{i=1}^N q_i(t) \phi_i(r) \tag{2}$$

where q_i is the time dependent response and ϕ_i are the uniform cantilever beam free-vibration mode shapes. The uniform cantilever beam mode shapes can be written as follows [18, 19, 23]:

$$\begin{aligned} \phi_i(r) = & \sin(\beta_i r) - \sinh(\beta_i r) \\ & - \left(\frac{\sin(\beta_i L) + \sinh(\beta_i L)}{\cos(\beta_i L) + \cosh(\beta_i L)} \right) (\cos(\beta_i r) \\ & - \cosh(\beta_i r)) \end{aligned} \tag{3}$$

where L is the beam length. Note that in case of cantilever beams $\cos(\beta_i L) \cdot \cosh(\beta_i L) + 1 = 0$, so that $\beta_1 L = 1.875104$. The mode shapes can be normalized such that, for all i and j ,

$$\int_0^L \phi_i \phi_j dr = \begin{cases} \eta, & \text{if } i = j, \\ 0, & \text{if } i \neq j. \end{cases} \tag{4}$$

Substituting the truncated series into the Euler–Lagrange partial differential equation results in:

$$\begin{aligned} \rho A \frac{\partial^2 q_1}{\partial t^2} \int_0^L \phi_1^2 dr + EI \cdot q_1 \int_0^L \frac{\partial^4 \phi_1}{\partial r^4} \phi_1 dr \\ = \int_0^L f(r, t) \phi_1(L) dr \end{aligned} \tag{5}$$

Therefore, a system of linear second order Ordinary Differential Equation (ODE) will be obtained. This

equation, which describes the transverse dynamic behavior of the beam, can be given as follows:

$$\frac{\rho AL}{4} \frac{\partial^2 q_1}{\partial t^2} + \frac{12.362361EI}{4L^3} q_1 = F(r, t) \tag{6}$$

Finally, it can be concluded that the dynamic properties of the system (which are shown in Fig. 1b) are as $K = 3.0906EI/L^3$, $M = 0.25\rho AL$ and $C = 2\zeta(K \cdot M)^{1/2}$. Note that ζ is the damping ratio.

2.2 Modeling the dynamic behavior of the vibratory system with impact damper

As illustrated in Fig. 1b, it is clear that when $|y - x| < d/2$, the impact mass moves freely at a constant speed without causing any collision (free flight of the impact mass). Therefore, differential equations of motion between impacts can be given by

$$\begin{cases} M\ddot{x} + C\dot{x} + Kx = 0 \\ m\ddot{y} = 0 \end{cases} \tag{7}$$

When contact occurs ($|y - x| \geq d/2$), an impulsive force acts on both of the impact mass and main mass. The elastic contact force in this investigation is described using the Hertzian contact concept. Based on the Hertzian model of contact, the following relationship holds between the Hertzian contact force (F_c) and the relative displacement of the impact mass and barrier:

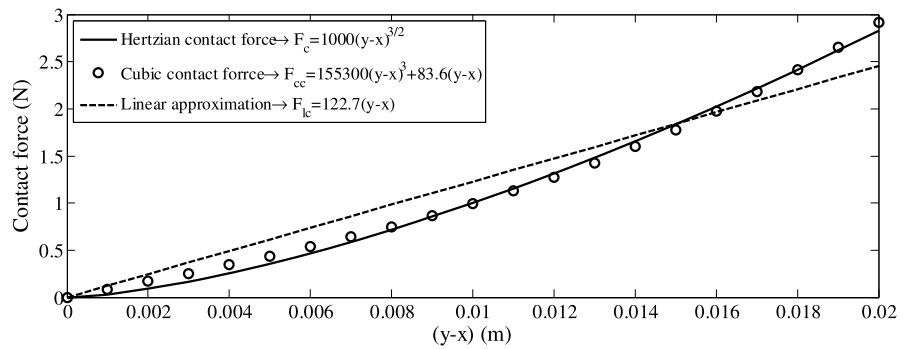
$$F_c = K_{Hz}(y - x)^{3/2} \tag{8}$$

where K_{Hz} is the Hertzian contact stiffness and y and x are the colliding masses displacements. In this investigation a new formulation for the Hertzian contact force is presented, which simply named cubic contact force. The so-called cubic contact force is given as follows:

$$F_{cc} = a(y - x)^3 + b(y - x) \tag{9}$$

where a and b are two constant coefficients, which depend on the Hertzian contact stiffness (K_{Hz}). Using the cubic contact force concept, the vibro-impact problems can analytically be studied. Comparison between the cubic and Hertzian contact forces is shown in Fig. 2. Furthermore, in this figure linear approximation of the Hertzian contact is shown in Fig. 2.

Fig. 2 Comparison between the Hertzian, cubic and linear contact forces



Note that, in the present study, the maximum value of the relative displacement is considered as 2 cm and the Hertzian contact stiffness is equal to $1000 \text{ N/m}^{3/2}$. The coefficients a and b in (Eq. (9)) can be obtained using the curve fitting toolbox of MATLAB software. As shown in Fig. 2, unlike the linear approximation, the cubic contact model can accurately be used instead the Hertzian contact model. Using the cubic contact force, the governing equations of the resilient impact damper system, when contact occurs ($|y - x| \geq d/2$), can be written as follows:

$$\begin{cases} M\ddot{x} + C\dot{x} + Kx - c_1(\dot{y} - \dot{x}) - a(y-x)^3 - b(y-x) = 0; \\ x(0) = X_0, \dot{x}(0) = \dot{X}_0 \end{cases} \quad (10.1)$$

$$\begin{cases} m\ddot{y} + c_1(\dot{y} - \dot{x}) + a(y-x)^3 + b(y-x) = 0; \\ y(0) = Y_0, \dot{y}(0) = \dot{Y}_0 \end{cases} \quad (10.2)$$

Note that the clearance (d) is indirectly considered in calculations, because the above equations describe the vibratory behavior of the discussed vibro-impact system, only when contact occurs and it happens if the relative displacement of masses is equal to (or greater than) half of the clearance ($|y - x| \geq d/2$).

2.3 Solving the problem

In this section the nonlinear differential equations of motion for the discussed vibro-impact system is theoretically investigated. To do this, initially, a simplified equivalent conservative vibratory system is investigated. Then, the equation of motion for the vibro-impact system is completely studied. In doing so, the solution method is divided to two parts:

- Finding a relation between the main mass displacement and the impact mass displacement, when they are connected to each other. In this part, for simplicity, the relative oscillation of the masses is considered undamped. The reason for this assumption lies in the fact that the contact duration, in reality, is very small and the damping term does not have a great effect on the relative oscillation of masses. Therefore, a relatively accurate relation between the main mass and impact mass displacements can be obtained without considering the damping properties.
- Solving the equation of relative motion for the impact and the main masses. In this part the damping term is considered in calculation and the equation of the relative motion is theoretically solved using perturbation method.

2.3.1 Main mass and impact mass displacements

General motion of the nonlinear versions of unforced vibratory systems is quasi-periodic [24]. This motion can be formulated by means of a finite Fourier series [25]. For simplicity, a series with a single harmonic component is considered as $x = A \cos \omega t$ and $y = B \cos \omega t$. Two coefficients A and B show the vibration amplitude of the main mass and impact mass motions, respectively. As a result, undamped form of the coupled ordinary differential equations (10.1) and (10.2) can be rewritten as follows:

$$\begin{cases} -M\omega^2 A \cos \omega t + KA \cos \omega t + a(A - B)^3 \cos^3 \omega t + b(A - B) \cos \omega t = 0 \end{cases} \quad (11.1)$$

$$\begin{cases} m\omega^2 B \cos \omega t - a(A - B)^3 \cos^3 \omega t - b(A - B) \cos \omega t = 0 \end{cases} \quad (11.2)$$

Note that the damping term will be accounted next in Sect. 2.4. The following relations can be obtained by vanishing of the coefficients of the secular term of Eqs. (11.1) and (11.2):

$$\begin{cases} -MA\omega^2 + KA + \frac{3a}{4}(A - B)^3 \\ + b(A - B) = 0 \\ -mB\omega^2 - \frac{3a}{4}(A - B)^3 - b(A - B) = 0 \end{cases} \quad (12)$$

Regarding to Eq. (12), the relation between the coefficients A and B is given by

$$\frac{B}{A} = \frac{K - M\omega^2}{m\omega^2} \quad (13)$$

Since $y = (B/A)x$, the undamped form of Eq. (10.1) is as follows:

$$\ddot{x} + \omega_0^2 x + \varepsilon x^3 = 0; \quad x(0) = X_0, \dot{x}(0) = \dot{X}_0 \quad (14)$$

where the frequency ω_0 and ε are as follows:

$$\begin{cases} \omega_0^2 = \frac{K}{M} + \frac{b}{M} \left(1 - \frac{K - M\omega^2}{m\omega^2}\right) \\ \varepsilon = \frac{a}{M} \left(1 - \frac{K - M\omega^2}{m\omega^2}\right)^3 \end{cases} \quad (15)$$

The Duffing equation, which is presented in Eq. (14), can be solved using the perturbation technique [26, 27]. In doing so, the expanded variable $x(x = x_0 + \varepsilon x_1 + \dots)$ and the expanded frequency ($\omega = \omega_0 + \varepsilon \omega_1 + \dots$) should be substituted into Eq. (14). It becomes

$$\begin{aligned} &(\ddot{x}_0 + \varepsilon \ddot{x}_1 + \dots) \\ &+ (\omega^2 - 2\varepsilon \omega_0 \omega_1 - \varepsilon^2 \omega_1^2 + \dots)(x_0 + \varepsilon x_1 + \dots)x \\ &+ \varepsilon x^3 = 0 \end{aligned} \quad (16)$$

The variable x_0 can be calculated by equating the coefficients of ε^0 to zero. Therefore the variable x_0 can be given by

$$\begin{aligned} x_0(t) &= \alpha \cos(\omega t + \beta); \\ \beta &= \tan^{-1}(-\dot{X}_0/\omega X_0), \alpha = X_0/\cos \beta \end{aligned} \quad (17)$$

Equating the coefficients of ε^1 to zero, the following relation will be obtained:

$$\ddot{x}_1 + \omega^2 x_1 = 2\omega_0 \omega_1 x_0 - x_0^3; \quad x_1(0) = \dot{x}_1(0) = 0 \quad (18)$$

Substituting Eq. (17) into Eq. (18) and vanishing the secular term leads to obtain the following relation:

$$\omega_1 = \frac{3}{8} \frac{\alpha^2}{\omega_0} \quad (19)$$

Regarding to Eq. (15) and Eq. (19), the following relation can be concluded:

$$\omega = \omega_0 + \frac{3}{8} \frac{a\alpha^2}{Mb^3\omega_0} (M\omega_0^2 - K)^3 \quad (20)$$

The frequency ω is the unknown of Eq. (13) and it can be calculated using the above relation. Remember that $y = (B/A)x$, so the relation between y and x can be obtained using Eq. (13) and Eq. (20).

2.3.2 The relative displacement

Relation between the impact mass displacement (y) and the relative displacement ($z = y - x$), can be written as $y = (B/(B - A))z$. Substituting the discussed relation into Eq. (10.2) leads to find the following relation:

$$\ddot{z} + \frac{B}{B - A} \left(\frac{c_1}{m} \dot{z} + \frac{a}{m} z^3 + \frac{b}{m} z \right) = 0 \quad (21)$$

Note that in the above relation, as said in Sect. 2.3, the damping term is accounted. For convenience, the above relation can be rewritten as follows:

$$\ddot{z} + \mu(\kappa_1 \dot{z} + \kappa_2 z^3) + \kappa_3 z = 0 \quad (22)$$

where the coefficients κ_1 , κ_2 , and κ_3 are equal to

$$\kappa_1 = \frac{B}{B - A} \frac{c_1}{\mu m}, \quad \kappa_2 = \frac{B}{B - A} \frac{a}{\mu m}, \quad \kappa_3 = \frac{B}{B - A} \frac{b}{m}$$

Equations (26.1), (26.2) can be solved using the two variable expansion method [24]. In doing so, the variable ξ represents stretched time ($\xi = \Omega t$), and η represents slow time ($\eta = \mu t$). In order to substitute η and ξ into Eq. (19), the first and second derivatives of the variable z with respect to t should be expressed using the chain rule:

$$\begin{cases} \frac{dz}{dt} = \Omega \frac{\partial z}{\partial \xi} + \mu \frac{\partial z}{\partial \eta} \\ \frac{d^2z}{dt^2} = \Omega^2 \frac{\partial^2 z}{\partial \xi^2} + 2\mu\Omega \frac{\partial^2 z}{\partial \xi \partial \eta} + \mu^2 \frac{\partial^2 z}{\partial \eta^2} \end{cases} \quad (23)$$

Substituting the above relations into Eq. (19) results in

$$\begin{aligned} \Omega^2 \frac{\partial^2 z}{\partial \xi^2} + 2\mu\Omega \frac{\partial^2 z}{\partial \xi \partial \eta} + \mu^2 \frac{\partial^2 z}{\partial \eta^2} \\ + \mu\Omega\kappa_1 \frac{\partial z}{\partial \xi} + \mu^2\kappa_1 \frac{\partial z}{\partial \eta} + \mu\kappa_2 z^3 + \kappa_3 z = 0 \end{aligned} \quad (24)$$

$$z(0) = 0, \quad \dot{z}(0) = \dot{Z}_0$$

The expanded variables of the above relation are as follows:

$$z = z_0 + \mu z_1 + \dots \quad (25.1)$$

$$\kappa_3 = \Omega^2 + \mu\Omega_1 + \dots \quad (25.2)$$

Note that in the case of impact damper systems, initial relative displacements of impact mass and main mass in each collision are equal to zero ($z(0) = 0$). Equating the same coefficients of μ to zero leads to find the following relations:

$$\frac{\partial^2 z_0}{\partial \xi^2} + z_0 = 0; \quad z_0(0) = 0, \dot{z}_0(0) = \dot{Z}_0 \quad (26.1)$$

$$\begin{aligned} \frac{\partial^2 z_1}{\partial \xi^2} + z_1 = -\frac{2}{\Omega} \frac{\partial^2 z_0}{\partial \xi \partial \eta} - \frac{\kappa_1}{\Omega} \frac{\partial z_0}{\partial \xi} \\ - \frac{\Omega_1}{\Omega^2} z_0 - \frac{\kappa_2}{\Omega^2} z_0^3; \end{aligned} \quad (26.2)$$

$$z_1(0) = \dot{z}_1(0) = 0$$

Regarding to Eq. (26.1) the variable z_0 can be calculated as $z_0 = N(\eta)\sin\xi$. Substituting z_0 into Eq. (26.2) and vanishing the coefficients of $\sin\xi$ and $\cos\xi$, results in

$$\frac{1}{\Omega} \left(2 \frac{dN}{d\eta} + \kappa_1 N \right) = 0 \quad (27.1)$$

$$\frac{1}{\Omega^2} \left(\frac{\Omega_1}{N^2} + \frac{3}{4}\kappa_2 \right) = 0 \quad (27.2)$$

Therefore, N and Ω_1 can be given by

$$N(\eta) = \frac{\dot{Z}_0}{\Omega} \exp\left(-\frac{\kappa_1}{2}\eta\right) \quad (28.1)$$

$$\Omega_1 = -\frac{3}{4}\kappa_2 N^2(\eta) \quad (28.2)$$

The circular frequency can be calculated by substituting Eq. (28.2) into Eq. (25.2). Therefore, the circular

frequency of relative motion of the colliding masses can be calculated as follows:

$$\Omega^2 = \frac{B}{B-A} \left(\frac{b}{m} + \frac{3a}{4m} \frac{\dot{Z}_0^2}{\Omega^2} \exp\left(-\frac{B}{B-A} \frac{c_1}{m} t\right) \right) \quad (29)$$

Note that, when the impact mass collides with the main mass, it stays in contact with the main mass for half the resonance period. The half the resonance period is conveniently named ‘‘contact duration’’. Therefore, the so-called contact duration (T_{CD}) can be formulated as follows:

$$\begin{aligned} T_{CD} = \pi \left[\frac{B}{B-A} \left(\frac{b}{m} + \frac{3a}{4m} \left(\frac{T_{CD}}{\pi} \right)^2 \dot{Z}_0^2 \right. \right. \\ \left. \left. \times \exp\left(-\frac{B}{B-A} \frac{c_1}{m} T_{CD}\right) \right) \right]^{-1/2} \end{aligned} \quad (30)$$

The contact duration can be calculated using the iteration technique. The iteration formula for the above relation can be written as follows:

$$\begin{aligned} T_{CD}^{(i)} = \pi \left[\frac{1}{1 - (B/A)^{-1}} \left(\frac{b}{m} + \frac{3a}{4m} \left(\frac{T_{CD}^{(i-1)}}{\pi} \right)^2 \dot{Z}_0^2 \right. \right. \\ \left. \left. \times \exp\left(-\frac{1}{1 - (B/A)^{-1}} \frac{c_1}{m} \right. \right. \right. \\ \left. \left. \left. \times T_{CD}^{(i-1)} \right) \right) \right]^{-1/2}; \quad i = 1, 2, \dots \end{aligned} \quad (31)$$

where the first iteration for the contact duration can be considered as $T_{CD}^{(0)} = 2\pi[(1 - A/B)(m/b)]^{1/2}$. After vanishing the secular term of Eq. (26.2) and mathematical calculations, the variable z_1 can be achieved. Regarding to Eq. (25.1) the relative displacement of the colliding masses can be formulated as follows:

$$\begin{aligned} z(\eta, \xi) = N(\eta) \cdot \sin(\xi) - \frac{aN^3(\eta)}{32m\Omega^2} \frac{B}{B-A} \\ \times [\sin(3\xi) - 3\sin(\xi)] \end{aligned} \quad (32)$$

When contact occurs, it can be concluded that the relation between the main mass displacement (x) and the relative displacement (z) is as follows:

$$x(\eta, \xi) = \frac{1}{(B/A) - 1} z(\eta, \xi) \quad (33)$$

Therefore, the main mass motion during the contact can be described using Eq. (33).

3 Equivalent linear contact duration and Hertzian contact duration

The contact duration depends on the stiffness and damping mechanism of the collided materials. The contact duration based on the Hertzian elastic contact has been obtained as follows [28]:

$$T_{CD}^{(Hertz)} = \frac{2.9432}{\dot{Z}_0^{0.2}} \left(\frac{5}{4K^*K_{Hz}} \right)^{2/5} \quad (34)$$

where $K^* = (m + M)/(m \cdot M)$. Furthermore, the contact duration has been calculated based on the linear model of the impact dampers [29]. The linear contact duration is given by

$$T_{CD}^{(Linear)} = \frac{2mM\pi}{\sqrt{m + M} \sqrt{4mMk_1 - c_1^2(m + M)}} \quad (35)$$

In the above relation, k_1 is the equivalent linear contact stiffness. For example, as shown in Fig. 2, if $K_{Hz} = 1000\text{N/m}^{1.5}$, the equivalent linear contact stiffness (k_1) is equal to 122.7 N/m.

4 Result and discussion

Variation of the parameter B/A , which is obtained in Sect. 2.3, with the main mass (M) is shown in Fig. 3a. As shown in this figure, for a low value of the mass ratio (m/M) the absolute value of the parameter B/A is relatively equal to M/m . But in high amounts of the mass ratio, the parameter B/A is related to the mass

ratio and stiffness of the main vibratory system (K). In the presented study, the so-called contact duration can be obtained using the iteration formula shown in Eq. (31). As shown in Fig. 3b, a relatively accurate value of the contact duration can be obtained after four iterations.

The calculated values for the contact duration, which are obtained using the perturbation method can be verified by the previous analytical results [28]. Furthermore, in the present study, the calculated results are compared with the linear solutions [29]. The results of this comparison are given in Table 1. As shown in this table, unlike the linear solution, accurate results can be obtained using the perturbation method.

A numerical example of the discussed vibro-impact system is given to clarify the theoretical calculations. In doing so, for the vibratory system shown in Fig. 1b, the nominal values of model parameters of the main vibratory system with the impact damper are considered as given in Table 2.

In this study, the dimensionless time is equal to $t' = t\sqrt{K/M}$. In the case of vibratory systems with impact dampers, decay of maximum displacement is initially linear and after a considerable decrease in displacement amplitude it is exponential. The initially linear decrease in the maximum displacement of the vibratory system with impact dampers is usually termed “damping inclination”, defined as follows [12]:

$$DI = (X_1 - X_2)/(t'_2 - t'_1) \quad (36)$$

where t'_1 and t'_2 are the dimensionless times of occurrence of the maximum positive displacements X_1 and X_2 respectively. In this study, the damping inclination

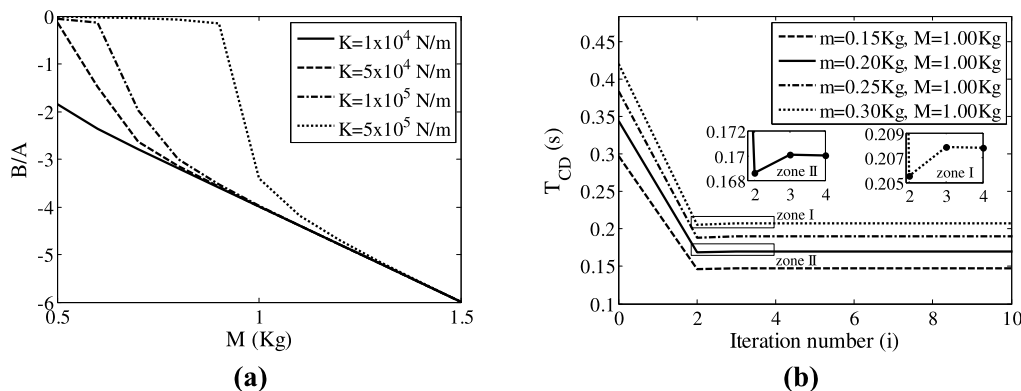


Fig. 3 Variation of B/A with M ($m = 0.25$ Kg, $a = 0.1553$ N/cm³, $b = 0.8360$ N/cm and $c_1 = 1$ Ns/cm) (a); Contact duration versus the number of iteration (b)

Table 1 Comparison between the equivalent linear and the cubic contact durations ($M = 1 \text{ kg}$ $K = 1000 \text{ N/m}$ and $\dot{Z}_0 = 7.5 \text{ cm/s}$)

$m \text{ (kg)}$	$M \text{ (kg)}$	Contact duration (s)		Error (%)
0.15	1.00	$T_{CD}^{(\text{Hertz})}$	0.1509	–
		T_{CD}	0.1407	6.76
		$T_{CD}^{(\text{Linear})}$	0.1024	32.14
0.20	1.00	$T_{CD}^{(\text{Hertz})}$	0.1664	–
		T_{CD}	0.1656	0.48
		$T_{CD}^{(\text{Linear})}$	0.1157	30.47
0.25	1.00	$T_{CD}^{(\text{Hertz})}$	0.1790	–
		T_{CD}	0.1885	5.31
		$T_{CD}^{(\text{Linear})}$	0.1268	29.16

Table 2 Parameters for the vibratory system with the impact damper system

Model parameters	$M = 1 \text{ kg}$ $K = 100 \text{ N/cm}$ $a = 0.1553 \text{ N/cm}^3$	$m = 0.25 \text{ kg}$ $c_1 = 5C = 5 \text{ N s/cm}$ $b = 0.8360 \text{ N/cm}$
Initial conditions	$\dot{X}_0 = 5 \text{ mm/s}$	$X_0 = Y_0 = \dot{Y}_0 = 0$

is considered as absolute value of the slop of the trend line passes through four initial maximum positive displacements of the main vibratory system. For example, for the vibro-impact system shown in Fig. 4, the damping inclination (DI) is equal to $71.05 \mu\text{m}$.

In the case of impact dampers, the impact mass collides with the main mass if the relative displacement of masses exceeds half of the clearance. Furthermore, it should be noted that an effective impact occurs if the impact mass and the main mass move toward each other. In other words, the impact is effective if the masses velocities are in opposite directions. Therefore, the necessary conditions for an effective collision can be given by

$$|y - x| \geq d/2 \quad \& \quad \dot{x} \cdot \dot{y} < 0 \tag{37}$$

Satisfying the effective contact condition ($\dot{x} \cdot \dot{y} < 0$), the maximum and minimum acceptable values of the gap sizes can be calculated. These values are illustrated in Fig. 5. As shown in this figure, for the presented vibro-impact system, values of the d_{\min} and d_{\max} are respectively equal to 6.49 mm and 34.43 mm . Each value between d_{\min} and d_{\max} is an acceptable gap size but usually it should be selected close to the minimum value of the acceptable gap sizes (d_{\min}).

The displacement response of the main mass for six different gap sizes is shown in Fig. 6. In this figure, two of the selected gap sizes (6 mm and 35 mm) are located out of the acceptable range. For convenience, these values are named as “out of range gap sizes” and the acceptable gap sizes are named “in range gap sizes”. Free vibration of the main vibratory system (when the impact mass moves between the barriers) can be easily determined using Eq. (7). During the contact, the formulation of the main mass motion is presented in Eq. (33). The main mass displacements (x) with several impact dampers are depicted in Fig. 6. As shown in this figure, using the out of range gap sizes, the impact damper system cannot strongly suppress vibration of the main mass.

As said before collision of the masses in an impact damper system is an effective impact if the colliding masses move toward each other ($\dot{x} \cdot \dot{y} < 0$). The total number of impacts (N_{tot}) and number of effective impacts (N_{eff}) with varying the gap size are listed in Table 3. In this table, variation of the damping inclination with the gap size is listed. The so-called “effectiveness” in Table 3 is defined as

$$\text{Effectiveness} = N_{\text{eff}} / (N_{\text{tot}} - N_{\text{eff}}) \tag{38}$$

Fig. 4 Waveforms of free vibrations without impact damper and with impact damper ($d = 9 \text{ mm}$)

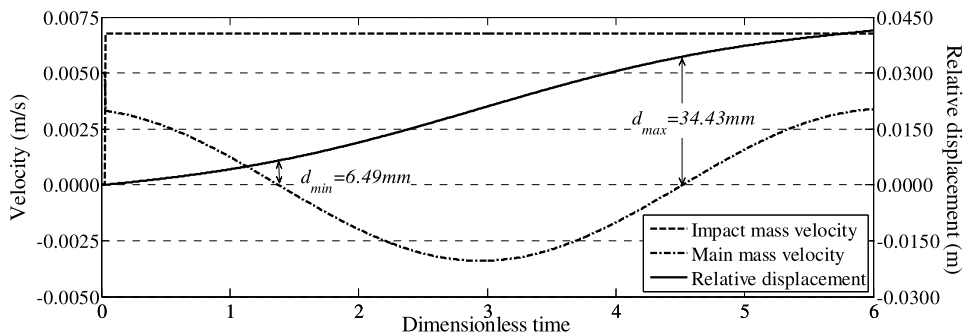
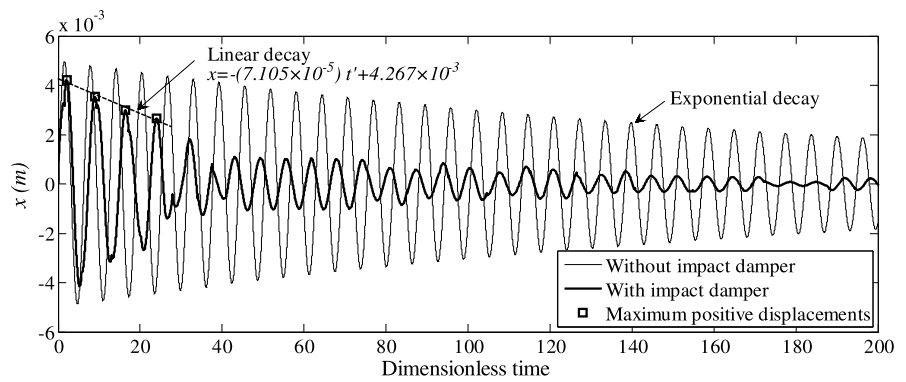


Fig. 5 The relative displacement between the main mass and the impact mass and velocities of them

Table 3 Total and effective number of impacts and final maximum displacement of the main mass

d (mm)	Gap size classification	N_{tot}	N_{eff}	Effectiveness	DI (μm)
6	Out of range	41	14	0.52	43.85
7	In range	24	13	1.18	64.56
9		19	11	1.38	71.05
15		12	7	1.40	82.40
20		19	10	1.11	43.55
25		9	6	2.00	88.72
32		12	6	1.00	61.60
34		10	6	1.50	75.32
35	Out of range	12	5	0.71	14.98

The effectiveness shows ratio of the effective impacts ($\dot{x} \cdot \dot{y} < 0$) to the non effective impacts ($\dot{x} \cdot \dot{y} > 0$).

As shown in Table 3, selecting the in range gap sizes for resilient impact damper systems usually lead to design strong impact dampers with higher damping inclinations. The variation of the effectiveness, number of effective impacts, and damping inclination with the gap size are shown in Fig. 7. As shown in this fig-

ure, unlike number of the effective impacts, the effectiveness can be used to predict the damping inclination behavior.

5 Conclusions

In the presented study, a mathematical model has been used to predict the strongly nonlinear behavior

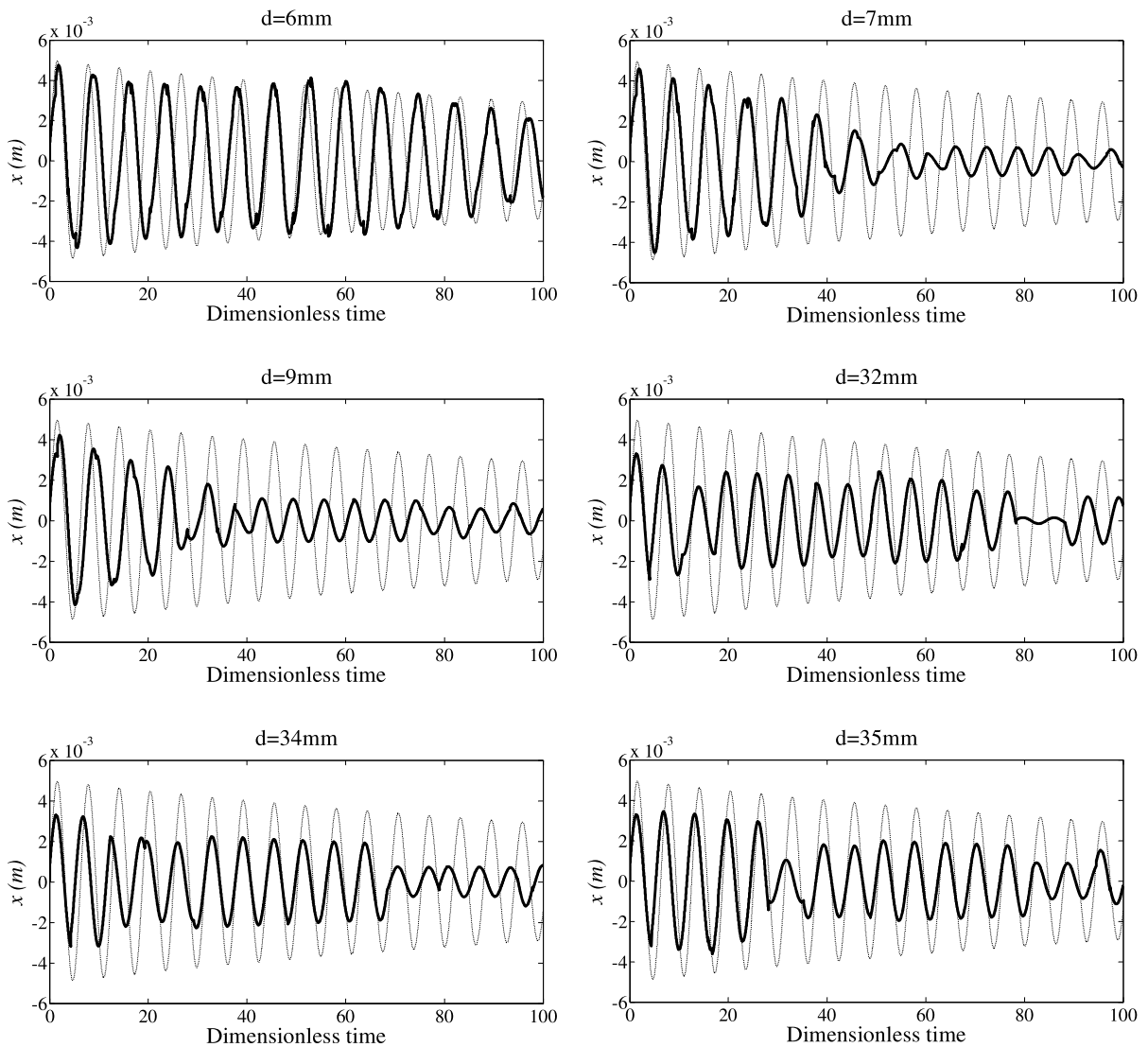


Fig. 6 Displacement responses of the main mass versus the dimensionless time with impact damper (—) and without impact damper (...)

of the impact damper systems in free damped vibrations. The presented model incorporates the Hertzian contact and constructed using spring, mass and viscous damper. The deformation of impact damper during the collision of the masses is accounted; therefore, the contact duration is taken into consideration.

The governing coupled nonlinear differential equations of the presented vibro-impact system are simplified using the nonlinear normal modes concept. The reduced nonlinear ordinary differential equations are solved using the perturbation method. The cal-

culated results are verified by the previous theoretical results. It is shown the presented solution method can increase accuracy of the solution up to 99 percents.

In the present study, based on the effective impact concept, the gap sizes are categorized as the “in range” and “out of the range” gap sizes. It is shown selecting the “in range” gap sizes for a resilient impact damper can increase the damping inclination up to 83 percents. Finally it is clearly shown that variation of the damping inclination is not depending on the number of ef-

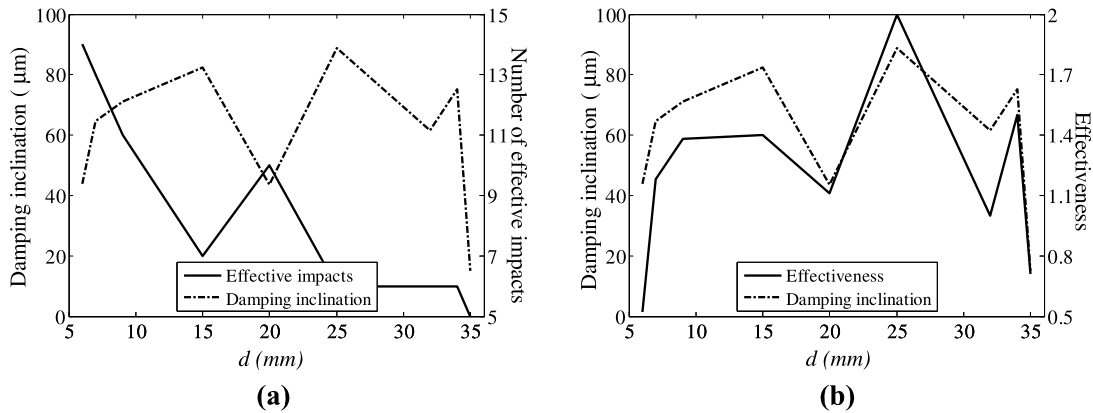


Fig. 7 Variation of the damping inclination and number of effective impacts with the gap size (a); Variation of the damping inclination and the effectiveness with the gap size (b)

fective impacts, but it is similar to variation of the so-called “effectiveness”.

References

1. Andreaus, U., Casini, P.: Dynamics of SDOF oscillators with hysteretic motion-limiting stop. *Nonlinear Dyn.* **22**(2), 145–164 (2000). doi:10.1023/a:1008354220584
2. Andreaus, U., Placidi, L., Rega, G.: Numerical simulation of the soft contact dynamics of an impacting bilinear oscillator. *Commun. Nonlinear Sci. Numer. Simul.* **15**(9), 2603–2616 (2010). doi:10.1016/j.cnsns.2009.10.015
3. Andreaus, U., Placidi, L., Rega, G.: Soft impact dynamics of a cantilever beam: equivalent SDOF model versus infinite-dimensional system. *Proc. Inst. Mech. Eng., Part C, J. Mech. Eng. Sci.* **225**(10), 2444–2456 (2011). doi:10.1177/0954406211414484
4. Dimentberg, M.F., Iourtchenko, D.V.: Random vibrations with impacts: a review. *Nonlinear Dyn.* **36**(2), 229–254 (2004). doi:10.1023/B:NODY.0000045510.93602.ca
5. Mann, B.P., Carter, R.E., Hazra, S.S.: Experimental study of an impact oscillator with viscoelastic and Hertzian contact. *Nonlinear Dyn.* **50**(3), 587–595 (2007)
6. Duncan, M.R., Wassgren, C.R., Krousgrill, C.M.: The damping performance of a single particle impact damper. *J. Sound Vib.* **286**(1–2), 123–144 (2005)
7. Ibrahim, R.A.: *Vibro-Impact Dynamics: Modeling, Mapping and Applications*. Lecture Notes in Applied and Computational Mechanics, vol. 43. Springer, Berlin (2009)
8. Popplewell, N., Liao, M.: A simple design procedure for optimum impact dampers. *J. Sound Vib.* **146**(3), 519–526 (1991)
9. Zhang, D.-G., Angeles, J.: Impact dynamics of flexible-joint robots. *Comput. Struct.* **83**(1), 25–33 (2005)
10. Zinjade, P.B., Mallik, A.K.: Impact damper for controlling friction-driven oscillations. *J. Sound Vib.* **306**(1–2), 238–251 (2007)
11. Blazejczyk-Okolewska, B.: Analysis of an impact damper of vibrations. *Chaos Solitons Fractals* **12**(11), 1983–1988 (2001)
12. Bapat, C.N., Sankar, S.: Single unit impact damper in free and forced vibration. *J. Sound Vib.* **99**(1), 85–94 (1985)
13. Ema, S., Marui, E.: A fundamental study on impact dampers. *Int. J. Mach. Tools Manuf.* **34**(3), 407–421 (1994)
14. Cheng, J., Xu, H.: Inner mass impact damper for attenuating structure vibration. *Int. J. Solids Struct.* **43**(17), 5355–5369 (2006)
15. Son, L., Hara, S., Yamada, K., Matsuhisa, H.: Experiment of shock vibration control using active momentum exchange impact damper. *J. Vib. Control* **16**(1), 49–64 (2010). doi:10.1177/1077546309102675
16. Andreaus, U., Casini, P.: Friction oscillator excited by moving base and colliding with a rigid or deformable obstacle. *Int. J. Non-Linear Mech.* **37**(1), 117–133 (2002). doi:10.1016/S0020-7462(00)00101-3
17. Andreaus, U., Chiaia, B., Placidi, L.: Soft-impact dynamics of deformable bodies. *Contin. Mech. Thermodyn.* **1**(24) (2012). doi:10.1007/s00161-012-0266-5
18. Palm, W.J.: *Mechanical Vibration*. Wiley, Hoboken (2007)
19. Rao, S.S.: *Vibration of Continuous Systems*. Wiley, Hoboken (2007)
20. Ba’zant, Z.P., Cedolin, L.: *Stability of Structures: Elastic, Inelastic, Fracture and Damage Theories*. World Scientific, Hackensack, London (2010)
21. Simitises, G.J., Hodges, D.H.: *Fundamentals of Structural Stability*. Elsevier/Butterworth-Heinemann, Amsterdam, Boston (2006)
22. Afsharfard, A., Farshidianfar, A.: An efficient method to solve the strongly coupled nonlinear differential equations of impact dampers. *Arch. Appl. Mech.* **82**(7), 977–984 (2012). doi:10.1007/s00419-011-0605-1
23. Thomson, W.T.: *Theory of Vibration with Applications*, 4th edn. Prentice Hall, Englewood Cliffs (1993)
24. Rand, R.H.: *Lecture Notes on Nonlinear Vibrations*. Cornell University, Ithaca (2005)
25. Kerschen, G., Peeters, M., Golinval, J.C., Vakakis, A.F.: Nonlinear normal modes, part I: a useful framework for the

- structural dynamicist. *Mech. Syst. Signal Process.* **23**(1), 170–194 (2009). doi:[10.1016/j.ymssp.2008.04.002](https://doi.org/10.1016/j.ymssp.2008.04.002)
26. Nayfeh, A.H.: *Introduction to Perturbation Techniques*. Wiley, New York (1981)
27. Nayfeh, A.H.: *Perturbation Methods*. Wiley Classics Library. Wiley, New York (2000)
28. Goldsmith, W.: *Impact: The Theory and Physical Behaviour of Colliding Solids*. Dover, Mineola (2002)
29. Cheng, C.C., Wang, J.Y.: Free vibration analysis of a resilient impact damper. *Int. J. Mech. Sci.* **45**(4), 589–604 (2003)